91-654
#1030060

DEPARTMENT OF NATIONAL DEFENCE

DEFENCE RESEARCH ESTABLISHMENT OTTAWA

CONTRACTOR REPORT DREO/PSD/EPS - 01/87

THERMAL EMISSIVITY OF ALUMINIZED PLASTIC FILMS (U)

By

N. McKay and T. Timusk

Department of Physics
McMaster University
Hamilton, Ontario
L8S 4M1

DREO Scientific Project Officer: Dr. Brian Farnworth

CONTRACT NO.: W7714-7-5324/01-5Z

DECEMBER 1987

DOCUMENT CONTROL DATA

(Security classification of title, body of abstract and indexing annotation must be entered when the overall document is classified)

1. ORIGINATOR (the name and address of the organization preparing the document. Organizations for whom the document was prepared, e.g. Establishment sponsoring a contractor's report, or tasking agency, are entered in section 8.)

Department of Physics
McMaster University
Hamilton, Ontario L8S 4M1

2. SECURITY CLASSIFICATION (overall security classification of the document. including special warning terms if applicable)

UNCLASSIFIED

3. TITLE (the complete document title as indicated on the title page. Its classification should be indicated by the appropriate abbreviation (S,C,R or U) in parentheses after the title.)

THERMAL EMISSIVITY OF ALUMINIZED PLASTIC FILMS (U)

4. AUTHORS (Last name, first name, middle initial)

McKAY, N. and TIMUSK, T.

5. DATE OF PUBLICATION (month and year of publication of document)

DECEMBER 1987

6a. NO. OF PAGES (total containing information. Include Annexes, Appendices, etc.)

41

6b. NO. OF REFS (total cited in document)

6

7. DESCRIPTIVE NOTES (the category of the document, e.g. technical report, technical note or memorandum. If appropriate, enter the type of report, e.g. interim, progress, summary, annual or final. Give the inclusive dates when a specific reporting period is covered.)

CONTRACTOR REPORT

8. SPONSORING ACTIVITY (the name of the department project office or laboratory sponsoring the research and development. Include the address.)

Defence Research Establishment Ottawa
National Defence
Ottawa, Ontario K1A 0Z4

9a. PROJECT OR GRANT NO. (if appropriate, the applicable research and development project or grant number under which the document was written. Please specify whether project or grant)

9b. CONTRACT NO. (if appropriate, the applicable number under which the document was written)

W7714-7-5324/01-5Z

10a. ORIGINATOR'S DOCUMENT NUMBER (the official document number by which the document is identified by the originating activity. This number must be unique to this document.)

CONTRACTOR REPORT DREO/PSD/EPS 01/87

10b. OTHER DOCUMENT NOS. (Any other numbers which may be assigned this document either by the originator or by the sponsor)

11. DOCUMENT AVAILABILITY (any limitations on further dissemination of the document, other than those imposed by security classification)

- (X) Unlimited distribution
- ( ) Distribution limited to defence departments and defence contractors; further distribution only as approved
- ( ) Distribution limited to defence departments and Canadian defence contractors; further distribution only as approved
- ( ) Distribution limited to government departments and agencies; further distribution only as approved
- ( ) Distribution limited to defence departments; further distribution only as approved
- ( ) Other (please specify):

12. DOCUMENT ANNOUNCEMENT (any limitation to the bibliographic announcement of this document. This will normally correspond to the Document Availabilty (11). However, where further distribution (beyond the audience specified in 11) is possible, a wider announcement audience may be selected.)

FINAL REPORT

on DSS Contract W7714-7-5324/01-5Z

THERMAL EMISSIVITY OF ALUMINIZED PLASTIC FILMS

N. McKay and T.Timusk
Department of Physics
McMaster University
Hamilton, Ontario
L8S 4M1

ABSTRACT

The thermal emissivity ε and related infrared optical properties are calculated for aluminum-backed polyester films in the range -40 to 100 °C using the frequency-dependent optical constants n and k for polyester measured in previous work. The aluminum layer is described by the Drude model, or treated as a perfectly-reflecting layer. Effects of multiple reflection and interference are fully included in the theory. Results for ε are presented as a function of the thickness both of the polyester (2 -30 μm) and of the aluminum layer. Calculations of the emitted radiation as a function of frequency and angle show that the apparent emissivity depends very little on viewing angle but is sensitive to the frequency response of the detector. A comparison with the measured emissivities of 10μm films shows fairly good agreement, with the calculated results about 10-20% higher.

INTRODUCTION

Heat is lost from insulated (or uninsulated) objects by convection, by conduction through still air or the insulation material, and by thermal infrared radiation. The effectiveness of an insulating layer depends on its ability to inhibit one or more of these modes of transport. Conduction can be reduced in lightweight materials by immobilising a thick layer of air. Thin materials have little effect on conductive heat loss, but can inhibit convection and radiative transfer.

Several manufacturers produce very thin polyester (Mylar) films for use as thermal insulation. In order to reduce radiative loss, these films are coated with a layer of aluminum, which is highly reflective in the infrared part of the spectrum. On the warm side of the material, the aluminum reflects most of the thermal radiation back to the warm object. On the cold side (the exterior surface if the insulation is keeping heat in) the aluminum emits much less infrared than the bare polyester film itself would, and the film therefore is kept at a somewhat higher temperature. Either of these effects may be important, depending on the situation.

In both cases the key parameter is the emissivity ε, defined as the power radiated per unit area from a surface divided by the same quantity for an "ideal" black surface at the same temperature. Measurements of ε for several samples

of aluminised polyester have been made by B. Farnworth at DREO, giving values for the polyester and aluminum side separately. In this report we describe calculations of the same quantities using the infrared optical constants of polyester from previous measurements (McKay,1984; McKay et. al.,1984, 1985). The aluminum is represented as a perfectly-reflecting surface, and more realistically by the simple Drude theory, which has been shown to be accurate for the part of the spectrum in which we are interested (Bennett & Bennett, 1966).

The theoretical results presented below provide a check on the measurements of ε, and show the effect of varying the physical parameters of the films. Results are given for the energy radiated from the surface as a function of the thickness of the polyester and the aluminum, and the variation with temperature and viewing angle is shown. We also display the absorption spectrum for the polyester side, and discuss the influence of the detector frequency response on measurements of ε for this surface.

THEORY

The problem of calculating the thermal radiation emitted from the surface of an aluminised polyester film after being generated throughout the bulk of the material and then experiencing reflections and refractions at the various interfaces is more easily approached by considering the absorption of radiation incident on the same surface from outside. It is well known from statistical physics that the radiation in an enclosed cavity in thermal equilibrium is isotropic and independent of the type of material lining the walls, and has an intensity and frequency spectrum which depend only on the temperature T. The condition of detailed balance requires that the radiation emitted by a surface held at a temperature T be equal to the power that would be absorbed at the surface from the radiation field in such a cavity, and that the equality must hold for each frequency and direction separately.

For the purpose of examining the transport of heat by thermal radiation, we are interested in the total power radiated from a surface element of unit area. This is conventionally written as

$$P = \varepsilon\sigma T^4 \qquad (2\text{-}1)$$

where σ is the Stefan-Boltzmann constant. This relation defines the emissivity ε, which contains all the information about the nature of the radiating surface. For an ideal black

surface which absorbs all incident radiation, ε is unity. For real materials ε is less than 1 and will depend on the characteristics of the radiating object and to some extent on the temperature.

The emissivity can be calculated from an appropriate average of the absorption properties of the surface over angle and frequency. Consider a surface element of area A with isotropic blackbody radiation incident on one side. A pencil of radiation arriving at an angle θ to the surface normal sees an effective cross-section of $A\cos\theta$, and the power striking A from directions in the solid angle element $d\Omega$ is

$$dP = I \cos\theta \, d\Omega \tag{2-2}$$

where the intensity I is independent of direction. Writing the absorptance (fraction of incident radiation absorbed) as $\alpha(\theta)$ and with $d\Omega = \sin\theta \, d\theta \, d\phi$, we integrate over the hemisphere to obtain

$$P = 2\pi I \int_0^{\pi/2} \alpha(\theta)\cos\theta \sin\theta \, d\theta. \tag{2-3}$$

For the case of an ideal black surface $\alpha = 1$ for all directions and frequencies. We can then integrate (2-3) and use (2-1) with $\varepsilon = 1$ to get

$$\pi I = \sigma T^4 \tag{2-4}$$

Substituting in (2-3) gives

$$\varepsilon = 2 \int_0^{\pi/2} \alpha(\theta) \sin\theta \cos\theta \, d\theta. \tag{2-5}$$

which defines ε in terms of α.

So far we have ignored the dependence of the intensity and the absorptance on the frequency f. We may write the frequency-dependent intensity $i(f)$ as

$$i(f) = I\ b(f) \tag{2-6}$$

where the normalised blackbody function b is

$$b(f) = B\ \frac{x^3}{(e^x - 1)} \tag{2-7}$$

Here B is a constant chosen so that

$$\int_0^\infty b(f) = 1 \tag{2-8}$$

and x is defined in terms of Planck's constant h and Boltzmann's constant k_B as

$$x = \frac{hf}{k_B T}\ . \tag{2-9}$$

We may write (2-3) in terms of the frequency-dependent functions $\alpha(\theta,f)$ and $i(f)$ as

$$P = 2\pi \int_0^\infty i(f) \int_0^{\pi/2} \alpha(\theta,f)\cos\theta\ \sin\theta\ d\theta\ df. \tag{2-10}$$

With the foregoing definitions, this leads to

$$\varepsilon = 2 \int_0^\infty b(f) \int_0^{\pi/2} \alpha(\theta,f)\cos\theta\ \sin\theta\ d\theta\ df. \tag{2-11}$$

To calculate the absorptance $\alpha(\theta,f)$ of a multilayer planar material we need to combine the Fresnel reflection and refraction coefficients at each interface with the absorption as the radiation propagates through each layer. Interference and multiple reflections can be included automatically by using a wave theory which considers the electric and magnetic

fields E and H in each layer rather than tracing the incident ray through an infinite series of reflections.

The propagation of electromagnetic radiation in an arbitrary (linear) nonmagnetic medium may be described entirely by the complex dielectric function $\varepsilon(f)$, or by the complex refractive index $m = n - ik$, with $m^2 = \varepsilon(f)$, and the complex square root taken so that k is positive ; this choice leads to attenuation along the direction the wave propagates (see, for example, Ginzburg, 1970). Plane wave solutions of Maxwell's equations in a medium then take the form

$$E(r,t) = E_0 \exp i\{2\pi f t - q \cdot r\} \qquad (2\text{-}12)$$

with

$$q^2 = (2\pi f m/c)^2 \qquad (2\text{-}13)$$

where the complex number q^2 is the sum of the squares of the components of q, and c is the speed of light in free space. Thus each component of the vector q is a complex number, which leads to attenuation of the wave represented by (2-12).

Consider the situation of fig. 1, with an infinite uniform slab to the right (positive z) side of the plane $z = 0$ and free space ($m = 1$) to the left. Radiation is incident from the left at an angle θ to the z-axis. We pick the plane of incidence to be the x-z plane, and for the moment consider transverse electric (TE) polarization, that is, only the y-component of E is nonzero. Suppressing the time-dependent factor $\exp i\{2\pi f t\}$ from all fields, we can write the incident beam as

$$E = E_R \exp -2\pi i\{ (f/c) [x \sin\theta + z \cos\theta] \} \qquad (2\text{-}14)$$

Because of the symmetry of the situation, the electric field everywhere must depend on x only through the overall factor exp $-i\{ 2\pi f/c \}$ of the incident field (2-14). Therefore the only other term in the field for the region $z<0$ must be of the form

$$E_L \exp -2\pi i\{ (f/c) [x \sin\theta - z \cos\theta] \} \qquad (2\text{-}15)$$

which describes a reflected wave with only the z-component of the wavevector reversed. The subscripts R and L have been chosen to represent right-going (incident direction) and left-going (reflected direction).

Similarly inside the slab, the field must have the form

$$E = E_R \exp\{-iQz \cos\theta\} + E_L \exp\{+iQz \cos\theta \} \qquad (2\text{-}16)$$

where now both the time-dependent and x-dependent exponential factors have been suppressed. The z-component of the wavevector q of (2-12) is represented as Q. In order to satisfy (2-13) we must have

$$Q = 2\pi(f/c) [m^2 - \sin^2\theta]^{1/2} \qquad (2\text{-}17)$$

with the imaginary part of the complex square negative for attenuated waves. This relation is true in each layer of the slab, with m and Q chosen for that particular layer, but θ always represents the incident angle of the beam at the top surface (that is, in air).

At this point we have the field throughout the slab as a function of position and time, with two parameters (E_L and E_R) for each layer. Applying boundary conditions on the fields E and H and their derivatives at each interface gives

the Fresnel formulae

$$E_{R,1} = \frac{Q_1 + Q_2}{2Q_1} E_{R,2} + \frac{Q_1 - Q_2}{2Q_1} E_{L2} \qquad (2\text{-}18a)$$

$$E_{L,1} = \frac{Q_1 - Q_2}{2Q_1} E_{R,2} + \frac{Q_1 + Q_2}{2Q_1} E_{L2} \qquad (2\text{-}18b)$$

The subscripts 1 and 2 refer to the media on the left and right sides of the interface, with refractive indices m_1 and m_2.

The transverse magnetic (TM) polarization is treated similarly, with the electric field E replaced by the magnetic field H. The resulting formulae are only slightly different :

$$H_{R,1} = \frac{Q_1 + (m_1/m_2)^2 Q_2}{2Q_1} H_{R,2} + \frac{Q_1 - (m_1/m_2)^2 Q_2}{2Q_1} H_{L2} \qquad (2\text{-}18c)$$

$$H_{L,1} = \frac{Q_1 - (m_1/m_2)^2 Q_2}{2Q_1} H_{R,2} + \frac{Q_1 + (m_1/m_2)^2 Q_2}{2Q_1} H_{L2} \qquad (2\text{-}18d)$$

More details are given in Ginzburg (1970) or other texts on advanced electrodynamics.

The fields at the left and right boundaries (but inside) a single layer are given by (2-16), if we let the two terms be represented by $E_R(z)$ and $E_L(z)$. Then

$$E_R(z) = E_R(0) \exp\{-iQz \cos\theta\} \qquad (2\text{-}19a)$$

$$E_L(z) = E_L(0) \exp\{+iQz \cos\theta\} \qquad (2\text{-}19b)$$

$$H_R(z) = H_R(0) \exp\{-iQz \cos\theta\} \qquad (2\text{-}19c)$$

$$H_L(z) = H_L(0) \exp\{+iQz \cos\theta\} \qquad (2\text{-}19d)$$

The equations (2-18) and (2-19) provide a systematic way of relating the incoming and outgoing amplitudes at the front and back faces of a multilayer slab. Because the boundary

conditions are specified at the rear face, we begin at the end by assuming a value of 1 (real) for the transmitted ray E_R or H_R just outside the slab. The left-going fields are zero here, since no radiation is incident from this side. Then equations (2-18) are used to obtain the L and R components on just inside the slab. In the case of radiation incident on the polyester side of an aluminised polyester film, this means just inside the surface of the aluminised side. Next, equations (2-19) give the field components at the polyester-aluminum interface (on the aluminum side). Equations (2-18) get us across into the polyester, equations (2-19) bring us to the front surface, and a final use of the Fresnel formulae gives the incident and reflected fields in the air, in terms of the arbitrarily chosen magnitude and phase of the transmitted radiation at the back surface. The transmission and reflection coefficients for the slab as a whole are determined by the ratios of the squared moduli of the field amplitudes, so the arbitrariness in this single parameter is not a problem. Using t and i subscripts for the transmitted and incident fields, we have for the transmission and reflection coefficients T and R

$$T = |E_{R,t}|^2 \; / \; |E_{R,i}|^2 \qquad (2\text{-}20a)$$

$$R = |E_{L,i}|^2 \; / \; |E_{R,i}|^2 \qquad (2\text{-}20b)$$

and

$$\alpha(\theta,f) = 1 - [\; T(\theta,f) + R(\theta,f) \;]. \qquad (2\text{-}21)$$

Similar relations for the TM mode are obtained by replacing E by H.

Other boundary conditions can be treated with similar ease. For an opaque aluminum layer, we require that no radiation arrives at the aluminum-polyester boundary from the right, so we set E_L and E_L to zero and E_R and E_R to 1 on the aluminum side of this interface. No radiation is transmitted in this case, of course, and the absorption is determined by comparing the incident and reflected intensities. Finally, for a perfectly-reflecting rear surface, we specify that the L and R amplitudes at the reflecting plane (but inside the polyester) are equal and the phases are equal for the magnetic fields, opposite for the electric fields. (This choice of phases is appropriate for reflection from a perfect conductor.)

RESULTS

At a temperature of 300K the characteristic frequency $k_B T/h$ is 208 cm^{-1} and the Planck function $b(f)$ in equation (2-7) has a broad peak at about 600 cm^{-1}. We are interested in the frequency region 100 - 2000cm^{-1}, which contains about 99% of the energy for blackbody radiation at this temperature. Values of the optical constants n and k for polyester in this frequency range have been reported previously (McKay et. al.,1984 ; McKay 1984). These measurements show strong absorption bands from 50 to 2000 cm^{-1}, with transparent regions at 500-700 cm^{-1} and at 1400-1600 cm^{-1}. Above 2000

cm^{-1} the material is transparent out to at least 2500 cm^{-1}. We have used these values for the calculations described here.

The calculated absorption for plain 10μm polyester film at normal incidence is plotted as a function of frequency in fig. 2. We see several well-defined peaks and a broad absorption band between 1000 and 1400 cm^{-1}, and the characteristic transparent windows at about 600 and 1600 cm^{-1}. These features are primarily due to the frequency variation of n and k, and appear in films of all thicknesses. Interference effects are generally not pronounced in strongly-absorbing layers.

Adding a perfectly-reflecting back to this film gives the behaviour in fig. 3. In general we see an increase in the absorption except in regions where where the absorption is nearly 100% to begin with. This is due to the radiation reflected from the back layer being absorbed on its way back to the front surface. In the plain polyester sheet, much of this escapes from the back and is not counted in the absorption. Of course, the apparent emissivity of partially-transparent materials may be affected by radiation passing through from the other side.

A more realistic treatment of the aluminum layer uses the Drude theory, in which the complex refractive index $m = n-ik$ is given in terms of the plasma frequency f_p and collision time γ by

$$m^2 = \frac{f^2 + (2\pi\gamma)^{-2} - i f_p^2/(2\pi\gamma f_p)}{f^2 + (2\pi\gamma)^{-2}} \quad . \qquad (3\text{-}1)$$

Bennett and Bennett (1966) report that this model accurately reproduces measured values of the surface reflectance of aluminum between 40 and 1400 cm^{-1}, using a value of f_p representing an electron density of 2.6 electrons/atom, and a value of γ derived from the dc conductivity. Converted to wavenumbers, these parameters are $f_p = 1.18 \times 10^5 cm^{-1}$, and $(2\pi\gamma)^{-1} = 654 cm^{-1}$. We have used this model for the rest of our calculations, but for a layer of opaque thickness (greater than about 200Å) there is little difference from the ideal perfectly-reflecting material. When the calculations shown in fig. 3 are repeated with a thick aluminum backing represented by the Drude model, the results are almost indistinguishable from each other on the scale of the graph.

Superimposed on fig. 3 is the blackbody spectral energy density function $b(f)$ for a temperature of 300K. Averaging the absorption with this frequency weighting gives the fraction of the energy absorbed from a beam of 300K thermal radiation incident normal to the surface. Alternatively, this average represents the apparent emissivity of the surface as measured by a detector which collects radiation only in this direction. In fig. 4, this frequency-averaged absorption is plotted as a function of angle. The intercept of all three curves at 0°represents the frequency average of the data in fig.3. At other angles, the TE and TM modes must be

calculated separately. Particularly at larger angles, the TM mode is more strongly absorbed. It is this mode which is refracted with no reflected component at the Brewster angle (for dielectric materials). The lower reflection at angles greater than about 60° leads to markedly higher absorption than for the TE mode.

The average of the two polarizations (solid curve) is more relevant to thermal transport and emissivity measurements. Since the factor of $\cos\theta$ in (2-2) is not included in these curves, the data represent the apparent emissivity (or relative brightness) of a large radiating surface when viewed from different angles. This brightness is nearly constant out to about 70°, as the increased reflectance at oblique incidence is partially balanced by the longer path that the rays take through the polyester film. This remains true for a much thicker film (26μm) as shown in fig. 5.

Averaging $\alpha(\theta,f)$ over a hemisphere with a factor of $\cos\theta$ as in (2-5) gives the spectra shown in fig. 6. Absorption for the TM mode (dashed curve) is generally higher than for the TE mode; the total emission or absorption of unpolarised radiation is simply the average of the two. Except for a moderate reduction in contrast between the peaks and valleys, this spectrum does not differ much from that of fig. 3, calculated for normal incidence only.

Integrating over both over directions and over frequencies as in (2-11) gives the true hemispherical emissivity ε, shown in table 1 and fig. 7 as a function of

film thickness for temperatures of -40°C, 20°C, and 100°C. The increase with temperature at a rate of 6 - 9x10^{-4}/°C occurs because the more strongly-absorbing regions above 900cm^{-1} in fig. 3 receive more weight in the frequency average at higher temperatures. For all three temperatures, ε increases steadily with thickness. At a thickness of about 8 μm, there is a dip in the absorption (or emissivity) probably because of an enhancement of the reflection at about 5cm^{-1} due to interference.

Table 2 lists measured values of thermal emissivity and reflectivity for several commercial materials. The first 5 samples listed show similar values (0.31 - 0.36) of emissivity on the polyester side, and low but variable emissivities (0.00 - 0.07) on the aluminized side. The sixth and seventh appear to be coated on both sides with a material of lower reflectivity, and we will not consider them further. The last sample is plain aluminum foil, which provides a useful reference point for the reflectances.

Dr. Farnworth of DREO, who provided these data, found the thickness of the fifth sample, "Becket Aluminized Polyester", to be 10 μm. Our data (table 1) predict an emissivity of 0.39 for the polyester side, about 10% higher than measured. The emissivity of the aluminized side (zero) is of course too low. Bennett and Bennett (1966) report a reflectance for aluminum that is nearly constant at 0.990 between 40 and 1400 cm^{-1}, and then drops to 0.980 at about 3000 cm^{-1}. Their measurements were made on opaque layers of

aluminum freshly deposited carefully polished optical flats in ultra high vacuum. They report that these reflectances are about 0.006 higher than the values for aluminum films prepared under "standard vacuum conditions". We would therefore expect reflectances no higher than about 0.98, and emissivities no lower than about 0.02. In general this is in agreement with the data in table 2 if we assume an uncertainty of about ±0.02. This is also suggested by the transmission coefficients obtained by subtracting the sum of the emissivity and reflectivity from 1 in table 2. These are about 0.02 -0.03 for the first five samples, but vary by amounts up to 0.04 for the same sample when calculated from the data for each side separately.

We investigated the effect of making the aluminum layer thin enough to be significantly transparent. The data shown in fig. 8 and table 3 are calculated for normal incidence only, but from the previous discussion we expect the behaviour to be very similar to an average over the entire hemisphere, and in any case direct measurements are generally made at or near normal incidence. For a thick back layer, the hemispherical average ε is 0.394 as compared to 0.406 at 0°, and the corrections to Table 3 ought to be similarly small.

Note that 1% transmission requires a thickness of no more than about 20Å for the aluminum layer. At this thickness, the absorption has increased to 0.510 from the value 0.406 for an opaque layer. This counterintuitive behaviour is due to the strong absorption of the radiation as

it passes through the metal. The nearly perfect reflection from a thick layer means that the field amplitudes inside the metal are very small. As the layer is made thin enough to be transparent, the fields inside the layer must become large, and consequently the dissipation increases. Of course, for a thin enough layer the absorption will decrease again, approaching that of the plain polyester film of fig. 1 in the limit of zero thickness. In the calculations, we found that this occurred only when the transmission reached 40% and the layer became less than 2Å thick.

DISCUSSION

We have presented results of calculations of the thermal emissivities and related infrared optical properties of aluminized polyester films for a wide range of film parameters. In order to compare our results with direct measurements made at DREO, we have concentrated on films 10μm thick and temperatures in the vicinity of 300K. For the thermal emissivity of a 10μm film with an opaque aluminum backing at 300K, we calculate a value 10 - 20% higher than that measured for a set of commercially-made materials. The measurements have an uncertainty of about 5% (± 0.02 in ε) judging from the scatter in the data. Further adjustments to the calculations will tend to increase, rather than decrease this discrepancy. The measurements collected radiation

primarily at right angles to the surface. As shown in fig. 4, this should yield a value slightly higher than the true hemispherical emissivity (0.40 instead of 0.39). If we adjust the thickness of the aluminum to give 1% transmission, the emissivity increases dramatically, due the strong attenuation of the wave in passing through the metallic layer. An adjustment of the frequency average to account for the detector response is also unlikely to reduce the apparent ε. The manufacturer's data on the infrared temperature measuring device used lists the response as 8 - 14μm or about 700 -1250 cm^{-1}. This lower limit tends to cut off part of the most transparent region of the spectrum (see fig. 3) and would result in higher readings for a polyester emitter. The actual value is very sensitive to the shape of the response curve. In the limit of a sharp cutoff at 700 cm^{-1} we would obtain a value of 0.56.

It is possible that the observed transmission through the films was due to imperfections (pinholes) in the aluminum layer. In this case we should take a weighted average of the emissivities of uncoated (0.27) and aluminised (0.40) polyester films. Since the transmission through a 10μm film is only 60%, a 2% total transmission implies about 3.5 % bare surface. This would reduce ε to 0.386.

In summary, the results of our calculations are approximately in agreement with the measurements, with the calculated emissivities being higher than the measurements by slightly more than the probable experimental uncertainty.

Of the various parameters that might be changed in the calculations, only a reduction in the thickness of the polyester would reduce the value of ε by a large amount. It would be useful to determine how uniformly the aluminum film covers the polyester and to measure its thickness. The shape of the spectral response curve of the detector, particularly near 600 cm^{-1}, could also have a sizable effect on the measured emissivities.

REFERENCES

Bennett, H.E. and Bennett, J.R. (1966), in Optical Properties and Electronic Structure of Metals and Alloys, edited by F. Abelès, North-Holland, Amsterdam.

Ginzburg, V.L. (1970), The Propagation of Electromagnetic Waves in Plasmas, 2nd edition, Pergamon Press, Oxford.

McKay, N.L. (1984), Ph.D. Thesis, McMaster University, Hamilton.

McKay, N.L., Timusk, T., and Farnworth, B. (1984), J. Appl. Phys. 55 (11) 4064.

McKay, N.L., Timusk, T., and Farnworth, B. (1985), in Thermal Conductivity 18 ,edited by T. Ashworth and D.R. Smith, Plenum, New York pp 393-402.

pp. 393-402

Table 1

Polyester film with opaque aluminum back

Film thickness, μm	Emissivity -40°C	20°C	100°C
2	.121	.171	.215
4	.205	.252	.298
6	.252	.305	.355
8	.268	.327	.384
10	.330	.388	.441
12	.360	.416	.468
14	.389	.444	.495
16	.414	.470	.521
18	.434	.489	.538
20	.461	.523	.560
22	.482	.533	.578
24	.496	.546	.590
26	.514	.562	.604
28	.533	.579	.619
30	.547	.591	.630

Table 2

Experimental data provided by B. Farnworth of DREO

Sample	Emissivity		Reflectivity	
	Shiny	Dull	Shiny	Dull
Taymor Emergency Blanket	.06	.31	.91	.65
Thermos Emergency Blanket	.02	.35	.95	.63
World Famous Emergency Blanket	.07	.33	.92	.63
Alouette Aluminized Mylar	.02	.34	.98	.62
Becket Aluminized Polyester	0.00	.36	1.00	.64
Thermos All-Weather Blanket	.16	.24	.81	.71
Alert Suit	.10	.10	.89	.83
Aluminum Foil	.02	.04	.97	.95

Table 3

300K thermal radiation at normal incidence on a 10 μm polyester film with an aluminum back layer

Thickness of Al layer (Å)	Absorption	Transmission	Reflection
10	0.575	0.043	0.382
12	0.558	0.032	0.410
14	0.543	0.025	0.433
16	0.530	0.020	0.450
18	0.519	0.016	0.465
20	0.510	0.013	0.477
30	0.478	0.006	0.515
40	0.460	0.004	0.536
50	0.449	0.002	0.549
60	0.441	0.0017	0.558
70	0.435	0.0012	0.564
80	0.430	0.0009	0.569
90	0.427	0.0007	0.572
100	0.424	0.0006	0.575
120	0.420	0.0004	0.580
150	0.415	0.0002	0.584
180	0.412	0.0001	0.587
200	0.411	0.0001	0.589
250	0.409	0.00006	0.591
300	0.407	0.00003	0.593
400	0.406	0.00001	0.594
500	0.406	0.000003	0.594

Fig. 1

Coordinate system for absorption by a slab.

Fig. 1

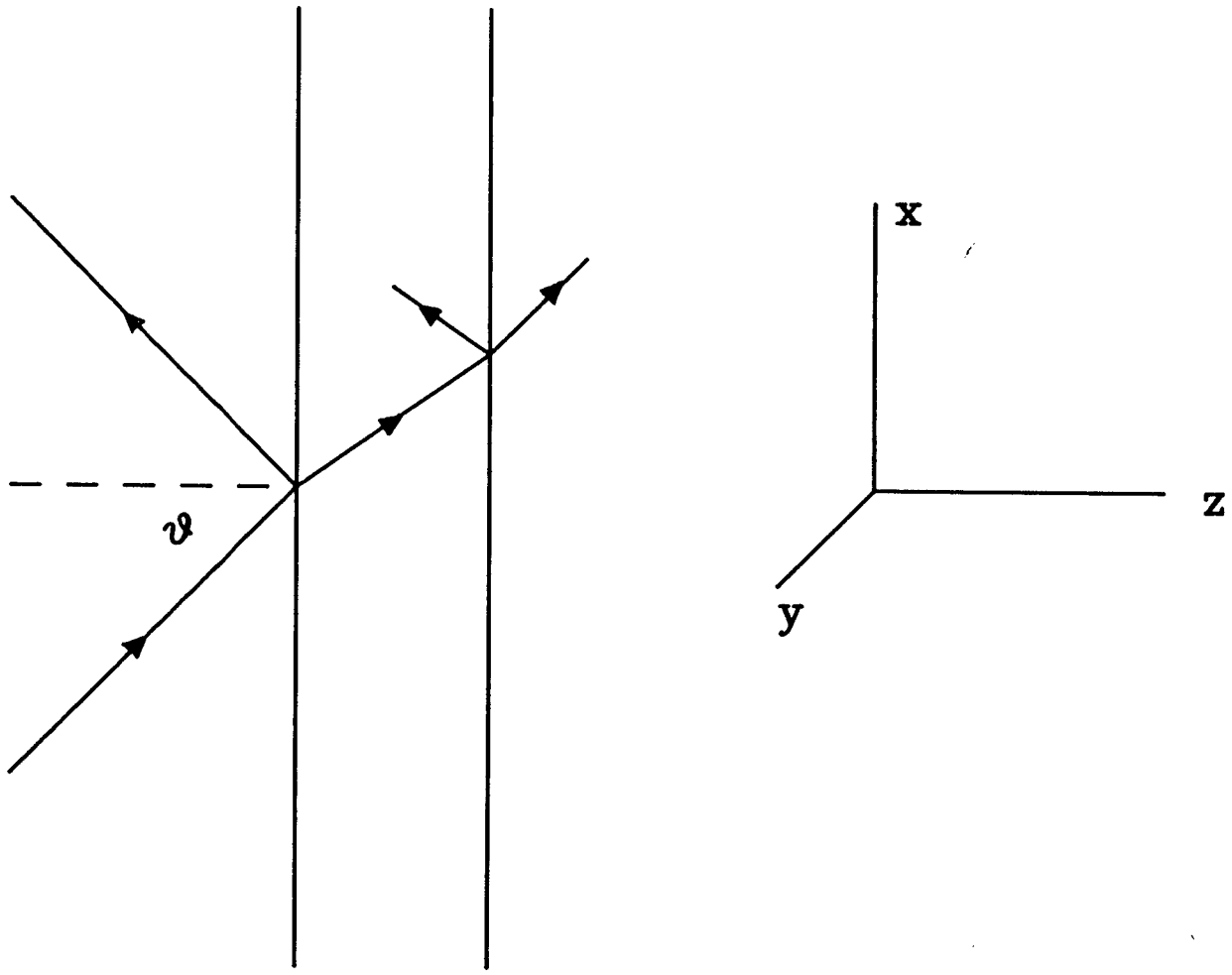

Fig. 2

Calculated absorption of a 10μm uncoated polyester film (normal incidence).

Fig. 2

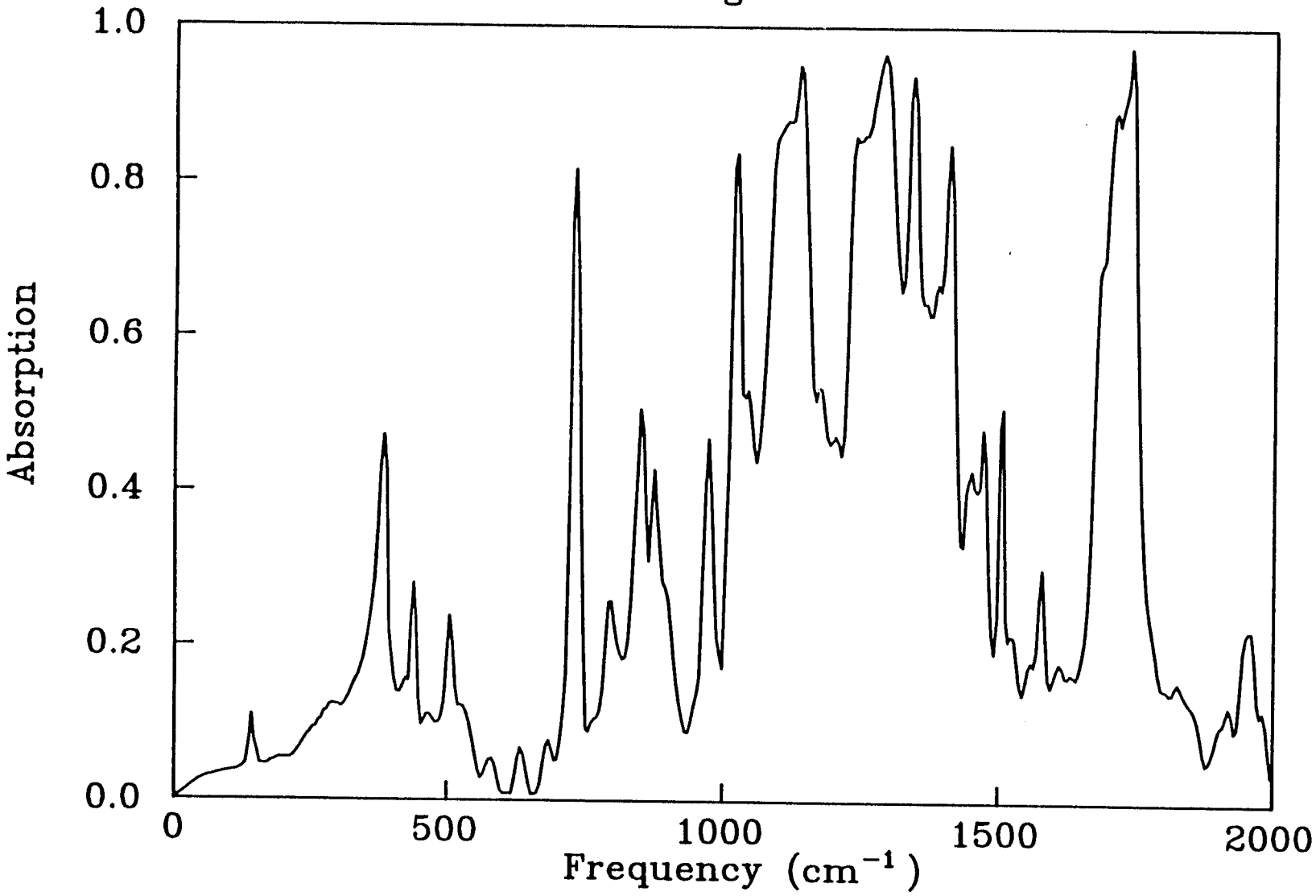
1.0
0.8
0.6
0.4
0.2
0.0
Absorption
0
500
1000
1500
2000
Frequency (cm⁻¹)

Fig. 3

Calculated absorption at normal incidence for a 10μm polyester film with a perfectly-reflecting backing. The dashed curve shows the shape of the blackbody spectrum at 300K.

Fig. 3

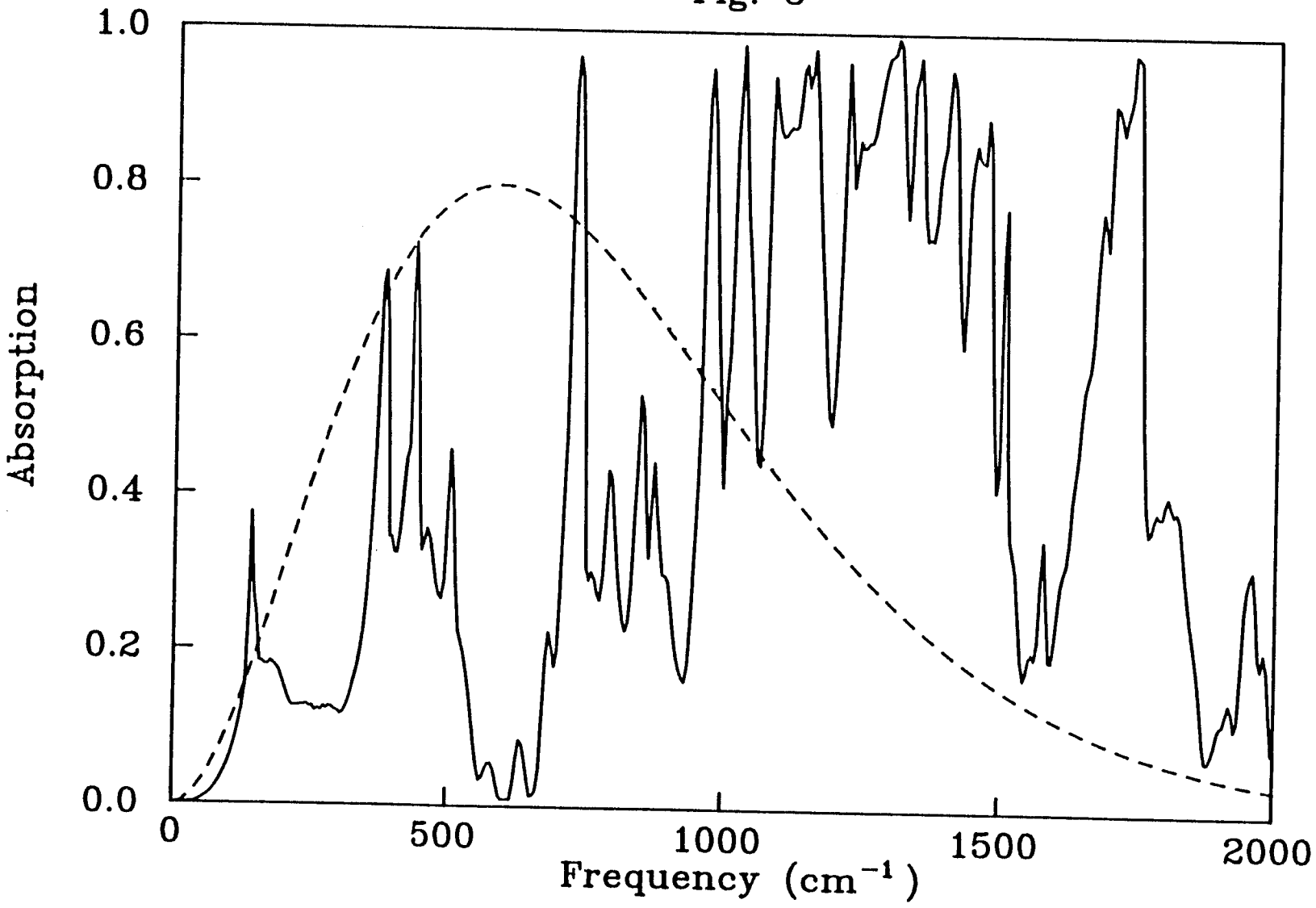
1.0
0.8
0.6
0.4
0.2
0.0
Absorption
0
500
1000
1500
2000
Frequency (cm^{-1})

Fig. 4

The absorptance $\alpha(\theta)$ for 10μm polyester film with an opaque aluminum back layer. The data have been averaged over frequency with a 300K blackbody function. The top and bottom cuves are for TM and TE polarisations respectively, and the solid curve represents unpolarised radiation.

Fig. 4

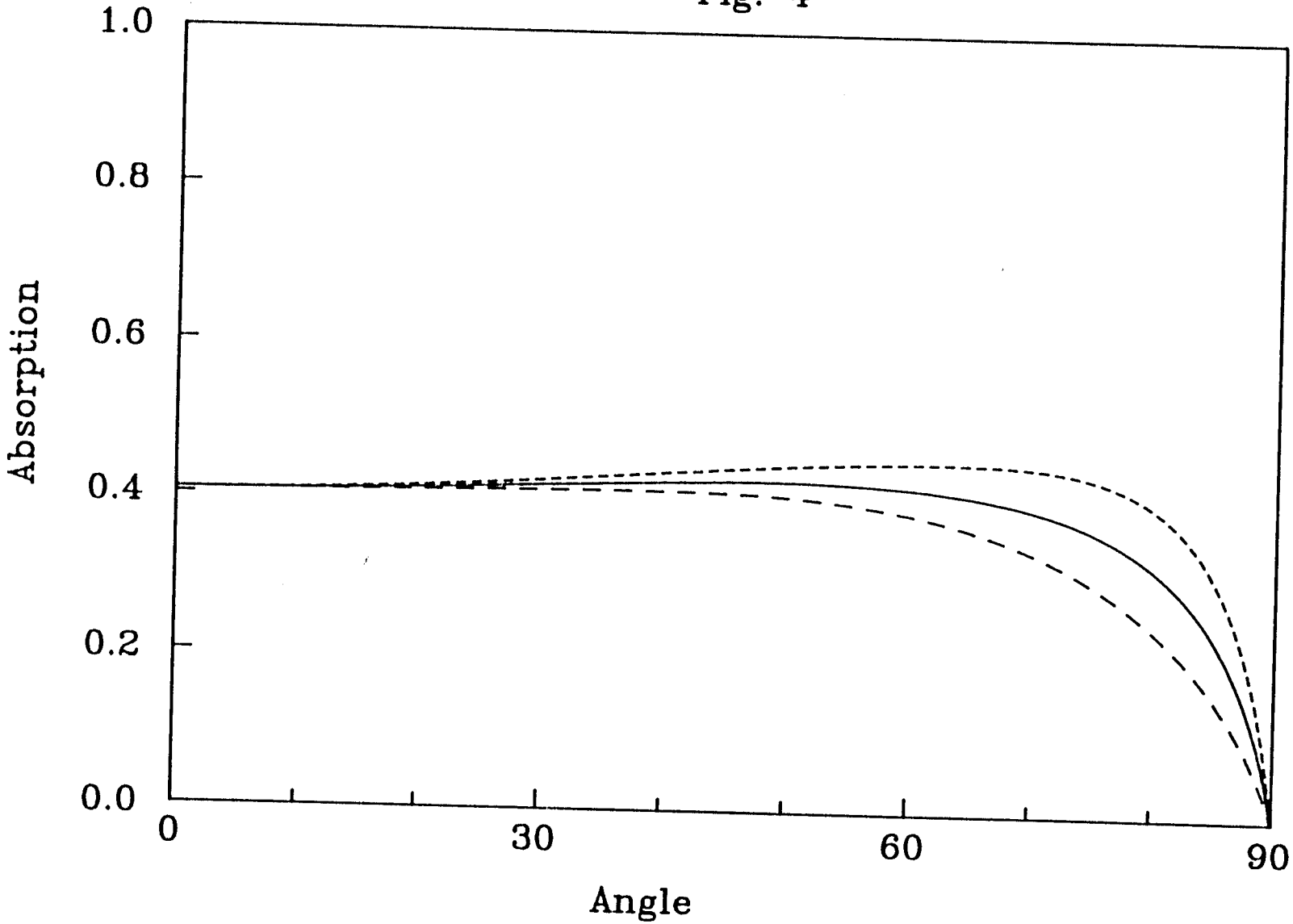

Fig. 5

The absorptance $\alpha(\theta)$ for 26μm polyester film with an opaque aluminum back layer. The data have been averaged over frequency with a 300K blackbody function. Frotop to bottom, the three curves represent TM, random, and TE polarisations.

Fig. 5

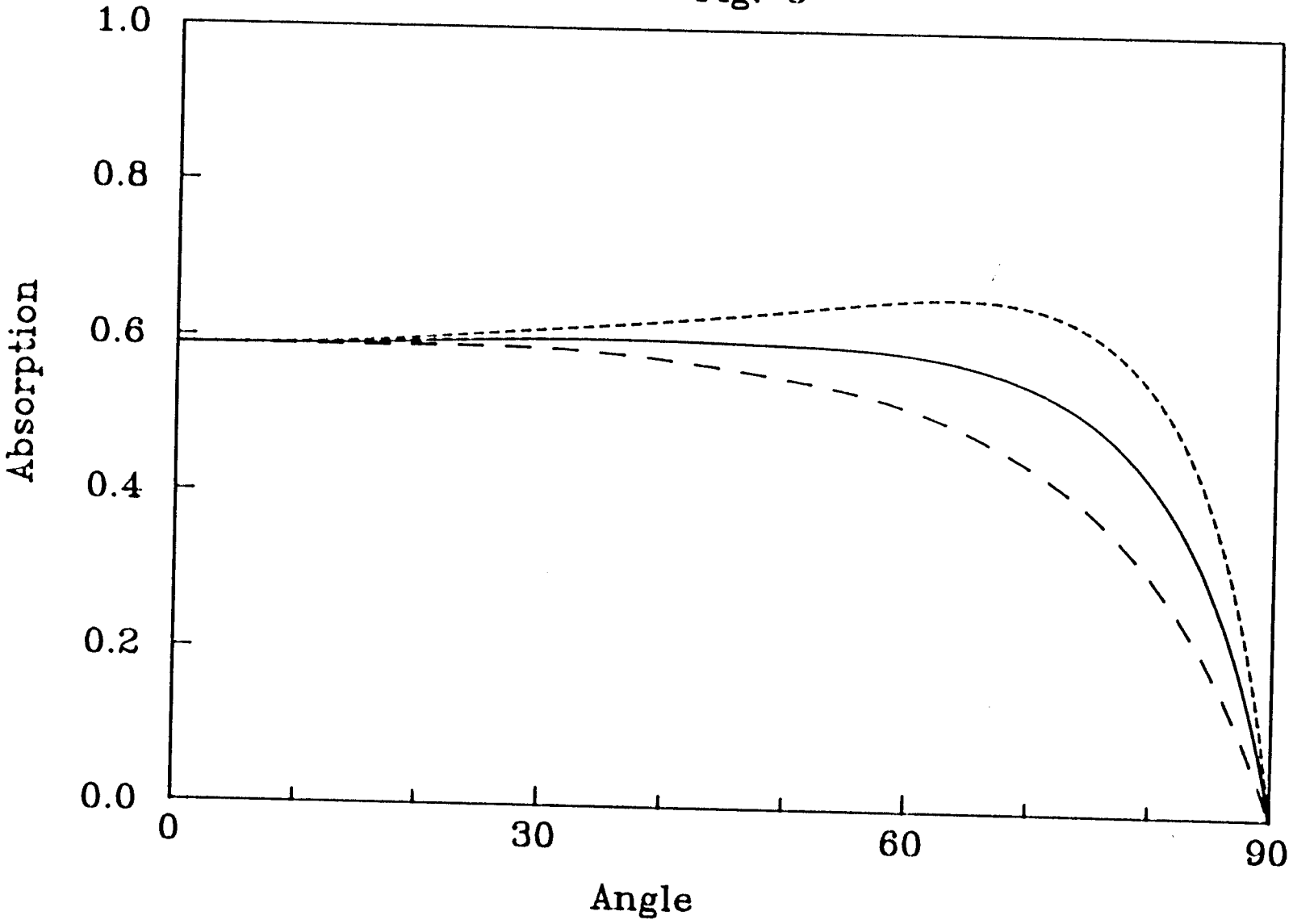

Fig.6

Absorptance averaged over incident angles for 10μm polyester with an opaque aluminum back. TE and TM modes are represented by solid and dashed curves respectively.

Fig. 6

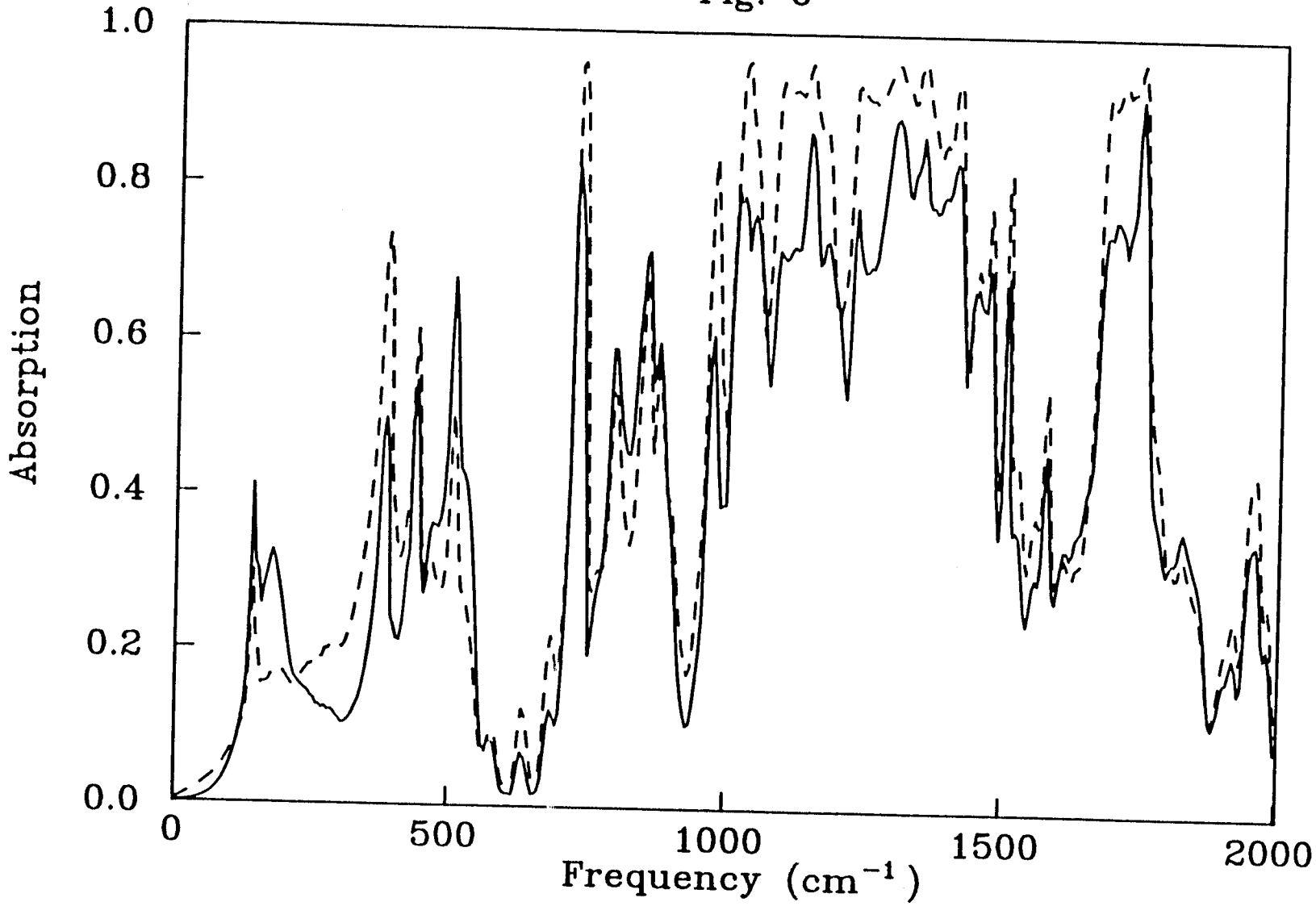
1.0
0.8
0.6
0.4
0.2
0.0
Absorption
0
500
1000
1500
2000
Frequency (cm^{-1})

Fig. 7

Calculated emissivity for polyester film with an opaque aluminum back. From top to bottom, the curves represent 100°C, 20°C, and -40°C .

Fig. 7

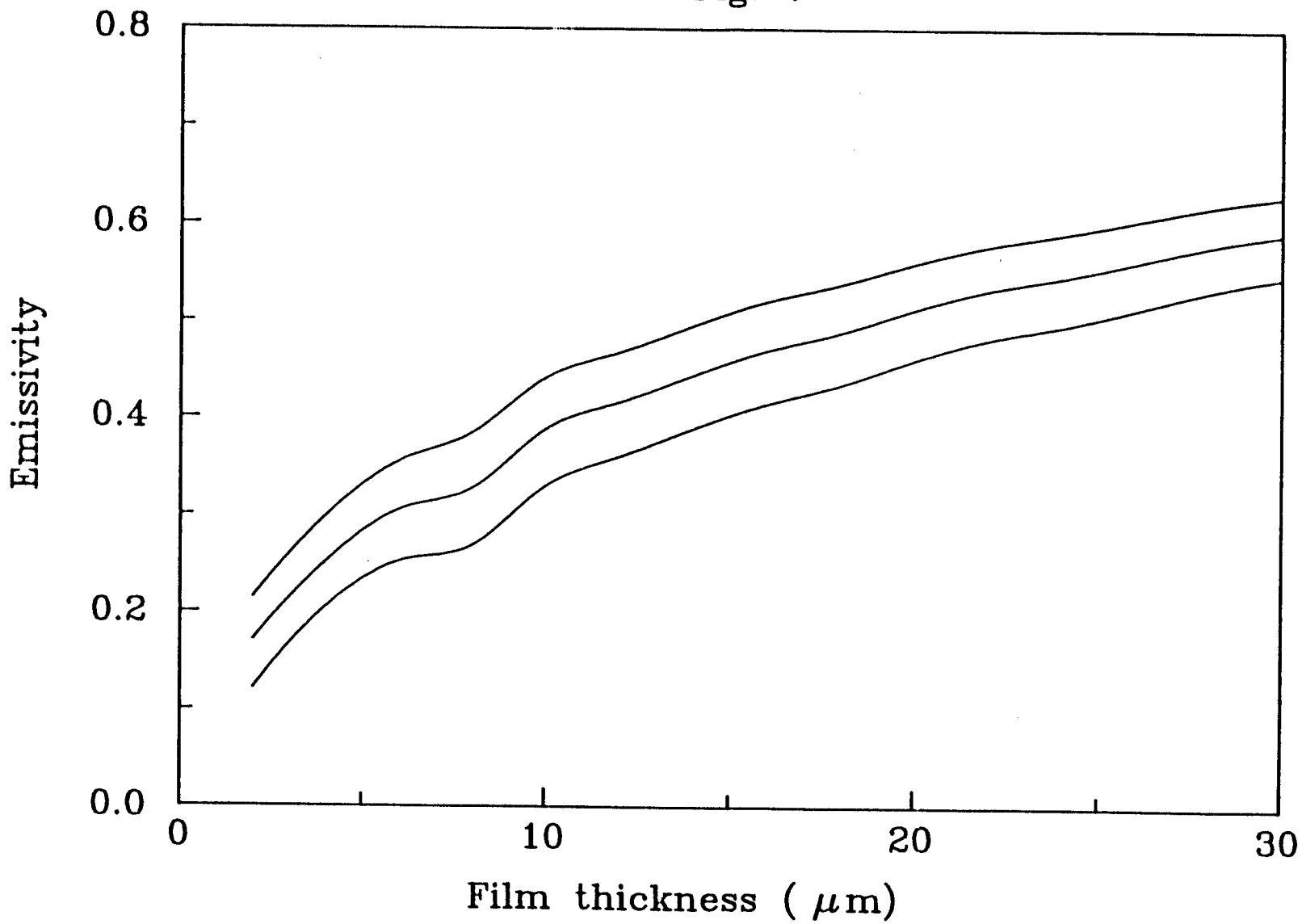

Fig. 8

Transmission at normal incidence for a 10μm polyester film with a thin aluminum back layer, plotted as a function of the thickness of the aluminum.

Fig. 8

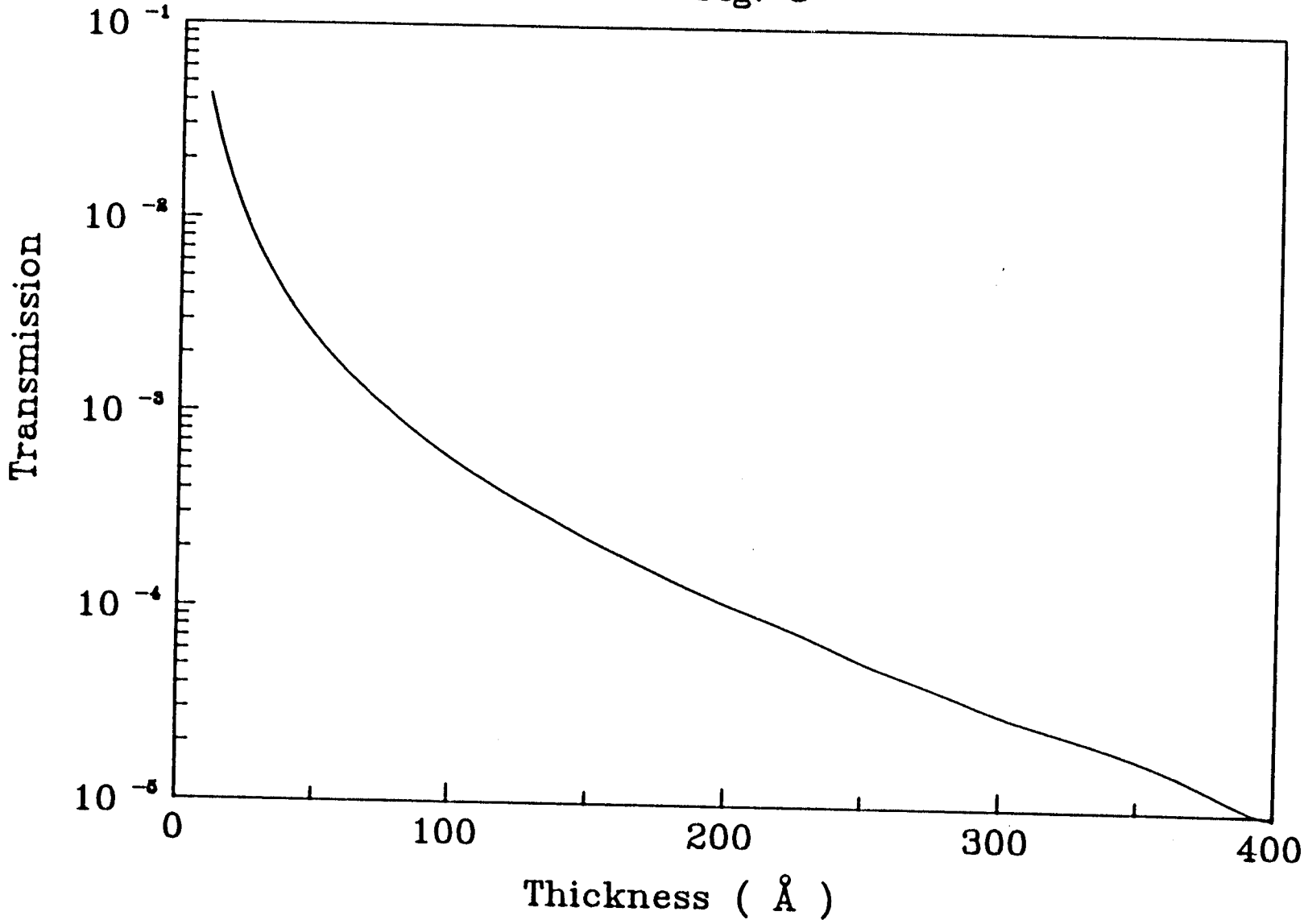
Transmission
10 -1
10 -2
10 -3
10 -4
10 -5
0
100
200
300
400
Thickness (Å)